Spatial tuning curves from apical, middle, and basal electrodes in cochlear implant users

David A. Nelson,[a] Heather A. Kreft, and Elizabeth S. Anderson
Clinical Psychoacoustics Laboratory, Department of Otolaryngology, University of Minnesota, MMC396, 420 Delaware St. S.E., Minneapolis, Minnesota 55455

Gail S. Donaldson
Department of Communication Sciences and Disorders, University of South Florida, PCD 1017, 4202 E. Fowler Ave., Tampa, Florida 33620

(Received 7 October 2010; revised 29 March 2011; accepted 30 March 2011)

Forward-masked psychophysical spatial tuning curves (*fm*STCs) were measured in 15 cochlear-implant subjects, 10 using monopolar stimulation and 5 using bipolar stimulation. In each subject, *fm*STCs were measured at several probe levels on an apical, middle, and basal electrode using a fixed-level probe stimulus and variable-level maskers. Tuning curve slopes and bandwidths did not change significantly with probe level for electrodes located in the apical, middle, or basal region although a few subjects exhibited dramatic changes in tuning at the extremes of the probe level range. Average tuning curve slopes and bandwidths did not vary significantly across electrode regions. Spatial tuning curves were symmetrical and similar in width across the three electrode regions. However, several subjects demonstrated large changes in slope and/or bandwidth across the three electrode regions, indicating poorer tuning in localized regions of the array. Cochlear-implant users exhibited bandwidths that were approximately five times wider than normal-hearing acoustic listeners but were in the same range as acoustic listeners with moderate cochlear hearing loss. No significant correlations were found between spatial tuning parameters and speech recognition; although a weak relation was seen between middle electrode tuning and transmitted information for vowel second formant frequency.
 [DOI: 10.1121/1.3583503]

PACS number(s): 43.66.Ts, 43.66.Lj, 43.66.Hg, 43.66.Dc [EB] Pages: 3916–3933

I. INTRODUCTION

The forward-masking spatial tuning curve (*fm*STC) was recently introduced to examine the spatial selectivity of electrical stimulation on individual electrodes in cochlear implant users (Nelson and Donaldson, 2002; Nelson *et al*., 2008). This procedure is modeled after a psychophysical forward-masking procedure that has been used to obtain frequency tuning curves in acoustically stimulated hearing (Houtgast, 1973; Moore, 1978; Vogten, 1978; Nelson, 1991; Moore and Alcantara, 2001). The forward masking paradigm makes use of a brief probe stimulus presented at a fixed, low current level (10%–30% of the dynamic range), presumably causing excitation of a narrow region of neural elements associated with the test electrode. Forward-masking is used to determine the masker level that just masks the probe for maskers presented to each electrode along the implanted array. The *fm*STC is a plot of the masker current level, on different electrodes across the electrode array, that is required to just mask the probe stimulus. Masker levels are typically lowest near the probe electrode and become increasingly higher at more distant locations, producing a tuning curve shape.

Nelson *et al*. (2008) measured *fm*STCs from each of 12 cochlear-implant users for a probe electrode near the middle of the electrode array. The *fm*STCs were obtained at several probe levels. Six subjects with the Advanced Bionics (Valencia, CA) C-I cochlear implant were stimulated in a monopolar electrode configuration, and six subjects with the Cochlear Corporation (Centennial, CO) Nucleus N-22 cochlear implant were stimulated in a bipolar electrode configuration. The resulting *fm*STCs were characterized by their apical and basal slopes (specified in dB/mm) and bandwidths measured 1 dB above the tip of the tuning curve (specified in mm). Apical and basal slopes were not significantly different from each other, i.e., spatial tuning curves were relatively symmetric, and the slopes were relatively independent of probe level. These findings are consistent with a linear "growth of response" in electric hearing, in contrast to the nonlinear growth of response in normal acoustic hearing (Nelson and Schroder, 1997; Nelson and Schroder, 1999; Nelson *et al*., 2001; Nelson and Schroder, 2004). Some individual subjects exhibited *fm*STCs that were mistuned, i.e., the tip of a spatial tuning curve was located at electrodes remote from the probe electrode, implying poor neural survival in the region of the probe electrode.

The present study extends our previous work to the assessment of apical and basal regions of the implanted array. A previous report of neural responses within the cochlea has indicated greater response amplitudes from apical regions relative to middle and basal regions (Frijns *et al*., 2002), leading to speculation about the effects of cochlear geometry on the spread of excitation across the cochlea (Kral *et al*., 1998). Related to this, an investigation of

[a]Author to whom correspondence should be addressed. Electronic mail: dan@umn.edu

 0001-4966/2011/129(6)/3916/18/$30.00

forward masking patterns in cochlear implant users has shown different shaped masking curves in different electrode regions (Cohen *et al*., 2003). To further investigate possible differences in spatial selectivity in different regions of the cochlea, the present study was undertaken to compare the characteristics of *fm*STCs from apical and basal electrodes with those reported previously for middle electrodes. It was anticipated that *fm*STCs in the apical and basal regions would exhibit the same *linear* behavior as observed for middle electrodes (Nelson *et al*., 2008), i.e., they would be symmetrical with slopes that are independent of probe level. To evaluate this hypothesis, *fm*STCs were obtained at multiple probe levels for apical, middle, and basal electrodes in each of 15 cochlear implant users.

II. METHODS

A. Subjects and electrodes

Subjects were 15 post-lingually deafened adults, 5 implanted with an Advanced Bionics C-I device (Schindler and Kessler, 1993; Kessler, 1999), 3 implanted with an Advanced Bionics C-II Bionic Ear device (Frijns *et al*., 2002), 2 implanted with an Advanced Bionics HiRes90K device, and 5 implanted with a Cochlear Corporation Nucleus N-22 device (Patrick and Clark, 1991). The Advanced Bionics users were implanted with a 16-electrode Spiral array (SPRL), a 16-electrode HiFocus array (HF), a 16- electrode HiFocus array with an electrode positioning system (HFP), a 16-electrode HiFocus array with an attached electrode positioning system (HF2), or the newer 16-electrode HiFocus "1j" (HF1j). The Nucleus users were implanted with a 22-electrode straight array. Table I displays relevant information for each subject including gender, age, etiology of deafness, duration of hearing loss prior to implantation, duration of implant use prior to participation in the study, electrode type (Advanced Bionics users), and insertion depth.

For each of the 15 subjects, an *fm*STC was obtained for a probe electrode near the middle of the array, a probe electrode near the base, and a probe electrode near the apex (see Appendix). Three probe levels were assessed at current amplitudes that were usually between 10% and 30% of the probe dynamic range in microamps (DRμA). A few subjects required higher probe levels to produce a sufficiently loud probe that was reliably detected when the masker was well below its masking level.

Advanced Bionics subjects were stimulated in monopolar (MP) mode. The Advanced Bionics Spiral electrode array (SPRL) incorporates eight lateral and eight medial electrodes with each lateral and medial electrode offset radially from the other. For this array, electrodes were numbered sequentially from 1 to 16 beginning with the most apical electrode; thus all odd-numbered electrodes were lateral electrodes and all even-numbered electrodes were medial electrodes. For subjects with the Advanced Bionics C-I receiver and SPRL array (C03 and C05), only medial electrodes were stimulated, which were separated by 2.0 mm. The Advanced Bionics HiFocus electrode array (HF) incorporates 16 electrodes in a linear arrangement; these electrodes were numbered 1–16 beginning with the most apical electrode. Subjects with the Advanced Bionics C-I receiver and HF array (C16, C18, and C23) were stimulated on the same electrodes used in their clinical speech-processor programs (either all even-numbered

TABLE I. Subject information.

Subject	M/F	Age	Etiology	Duration (yr)	CI use (yr)	Device (electrode type)	Depth (mm)	Consonant (%C)	Vowel (%C)	Sentences in quiet (%C)	Sentences in noise (%C)
C03	F	53.4	Progressive, familial	27	4.2	C-I (SPRL)	25	82.7	90.3	70.6	48.2
C05	M	47.8	Unknown, sudden	<1	5.6	C-I (SPRL)	25	77.0	90.3	70.2	18.6
C16	F	50.1	Progressive	13	2.6	C-I (HF)	25	80.8	83.0	60.8	15.2
C18	M	71.4	Otosclerosis	33	4.6	C-I (HFP)	25	63.4	49.6	26.6	1.6
C23	F	42.7	Progressive	27	1.1	C-I (HFP)	25	27.2	40.0	3.6	0.4
D02	F	58.2	Unknown	1	6.4	C-II (HF2)	25	62.6	92.7	43.8	7.6
D05	F	78.2	Unknown	3	6.6	C-II (HFP)	25	58.9	82.7	56.5	12.5
D08	F	54.7	Otosclerosis	13	3.8	C-II (HF)	25	75.6	58.8	24.8	12.0
D19	F	48.2	Unknown	7	3.5[a]	HiRes90K (HF)	25	70.5	86.7	76.0	35.8
D26	F	50.5	Unknown	7	1.9	HiRes90K (HF1J)	25	75.2	91.5	71.4	34.6
N13	M	65.2	Progressive, familial	4	12.8	N-22	24	68.8	80.9	28.6	8.6
N14	M	58.0	Progressive	1	8.4	N-22	25	67.8	89.9	61.0	29.8
N28	M	65.6	Meningitis	<1	8.6	N-22	25	43.4	57.6	14.8	0.6
N32	M	37.2	Maternal rubella	<1	7.4	N-22	23	72.4	84.2	53.2	6.6
N34	F	57.9	Mumps, progressive	9	4.4	N-22	22	44.5	62.4	7.2	4.0

Gender, age when tested, etiology of deafness, duration of bilateral severe-to-profound hearing loss prior to implantation, duration of implant use prior to the study, implanted device with electrode type (SPRL, spiral; HF, HiFocus; HFP, HiFocus with positioner; HF2, HiFocus with attached positioner; HF1j, HiFocus1j) for Advanced Bionics users only, and insertion depth. Speech scores for each subject are shown as percentage correct (%C) for consonants, vowels, and sentences in quiet and in noise. The SNR for sentences in noise was +10 dB.

[a]D19 had 3.5 yr experience with the C-II device in her left ear. She was previously implanted with a C-I device in that same ear. Total implant use in the left ear was approximately 8 yr at the time this experiment started.

or all odd-numbered electrodes), which were separated by 2.2 mm. The remaining electrodes were not used because lack of regular stimulation resulted in high electrical impedances. Subjects with the Advanced Bionics C-II and HiRes90K were stimulated on all available electrodes (14–16 electrodes depending on the subject). Electrodes were separated by 1.1 mm for those with the HF (D08, D19), HFP (D05), or HF1J arrays (D26) and by 0.9 mm for those with the HF2 array (D02). These subjects will collectively be referred to as the C-II group from this point forward.

Nucleus N-22 subjects were stimulated in bipolar mode, using an electrode separation of 0.75 mm (BP), or the narrowest separation greater than 0.75 mm [either 1.5 mm (BP+1) or 2.25 mm (BP+2)] that allowed adequate loudness to be achieved at current amplitudes that could be produced by the device. Electrodes were numbered sequentially, beginning with the most apical electrode. Because this electrode-numbering scheme differs from that used clinically, electrode numbers (for all devices) were specified using the prefix "rEL," to indicate research electrode numbering.

These subject groups primarily represent two types of electrode configurations. The C-I and C- II subjects were stimulated in a monopolar mode, while the N-22 subjects were stimulated in a bipolar mode. C-II subjects could have been stimulated in a bipolar mode, but they preferred the monopolar mode for their clinical maps. The current research design elected to evaluate the electrode configuration used daily by each user; this was the mode used to evaluate speech perception in each user. Although a primary difference between groups was the electrode configuration, there were also differences in electrode architectures that could influence spatial selectivity. The present study was not intended to directly compare electrode configurations, which requires a within-subjects research design (Kwon and van den Honert, 2006). Rather, our goal was to examine tuning in different electrode regions across a somewhat diverse group of cochlear implant users.

B. Tuning-curve procedures

1. Stimuli

Advanced Bionics subjects were stimulated with trains of 500-Hz biphasic current pulses that had a per-phase duration of 75 μs (C-II) or 77 μs (C-I) and no delay between phases. Stimulus amplitudes were adjusted in clinical amplitude steps, called *stimulus units* or SUs, which are logarithmic amplitude steps of 0.15-0.30 dB; where decibel is calculated as $20*\log_{10}$(amplitude ratio). SUs were later specified as calibrated current amplitudes in microamps (μA) using look-up tables developed in our laboratory. The calibrated amplitudes compensate for nonlinearities in the current source that vary with electrode impedance and pulse rate. Electrode impedances were measured at the beginning and end of each data collection session.

Nucleus N-22 subjects were stimulated with trains of 500-Hz biphasic current pulses, which were cathodic first (relative to the active electrode) with a per-phase pulse duration of 200 μs and an interphase delay of 44 μs. Stimulus amplitudes were specified in clinical amplitude steps, called *current step units* or CSUs, which are amplitude steps that vary between 0.07 and 0.30 dB for the range of current amplitudes used here. CSUs were converted to calibrated current amplitudes in microamps (μA) using subject-specific tables provided by Cochlear Corporation.

2. Absolute thresholds and maximum acceptable loudness levels

Prior to obtaining *fm*STCs for a given probe electrode, absolute detection threshold (THSp) and maximum acceptable loudness level (MALp) were determined for the 10-ms probe pulse train. THSp was measured with a three-interval forced choice (3IFC) adaptive procedure similar to that used for measuring masked thresholds (described in the following text), but only one interval contained the probe stimulus and the other two contained silence. MALp was measured with an ascending method of limits procedure in which pulse trains, presented at a rate of 2/s, were slowly increased in amplitude until the subject indicated that loudness had reached a "maximum acceptable" level. Estimates for two consecutive ascending runs were averaged to obtain a single measure of MALp. THSp and MALp were measured at the start of each test session for the probe electrode to be evaluated in that session, and THSp was measured again at the end of the test session to screen for potential auditory fatigue effects. Corresponding measures of threshold (THSm) and maximum acceptable loudness level (MALm) were obtained for all masker electrodes, using the 160-ms masker pulse train. These measures were obtained both before and after the measurement of a series of *fm*STCs at different probe levels. The values of THSm and MALm reported here represent the average of at least six measures obtained across data collection sessions for a given subject.

The values of THS and MAL, and the masked thresholds of the *fm*STCs, are plotted on a linear current scale because loudness matching experiments between acoustic and electric hearing in the same subjects have demonstrated a linear relation between acoustic decibels and electric current (Zeng and Shannon, 1992). The use of the decibel scale is appropriate in acoustic hearing because cochlear nonlinearities produce logarithmic transforms between stimulus amplitudes and loudness percepts, i.e., equal-loudness changes are proportionate to equal-ratio changes in stimulus amplitude (acoustic sound pressure). The electrical system is more nearly a linear system because the nonlinearities of the cochlea are not present. In electric hearing, equal loudness changes are more proportional to linear amplitude changes than to equal amplitude ratios (except at near threshold amplitudes). Thus the use of a decibel scale would misrepresent perceptual equivalence. In particular, because a decibel scale compresses high current amplitudes and expands lower current amplitudes, it would inappropriately minimize differences in MAL across the cochlear array and inflate differences in THS across the array.

3. Adaptive masked-threshold procedure

Forward-masked (masker-level) thresholds were obtained using a 3IFC adaptive procedure. The masker pulse

train was presented in each of three listening intervals. The probe pulse train was presented in one of the three intervals, chosen randomly from trial to trial, with a 20-ms gap between the offset of the masker and the onset of the probe. The subject's task was to choose the "different" interval by pressing the appropriate button on a three-button computer mouse or by selecting one of three colored squares on a video screen using a standard mouse. Stimulus intervals were cued on the video screen, and correct-answer feedback was provided after each trial. The amplitude of the masker pulse train was initially set to a level 2–4 dB below the anticipated masked threshold. Masker amplitude was adjusted on subsequent trials using a two-up, one-down stepping rule that estimated the stimulus level corresponding to 70.7% correct discrimination (Levitt, 1971). For the first four reversals (in the direction of amplitude changes), the masker level was varied in 1 dB steps (0.5 dB steps in a few subjects with very small dynamic ranges). These initial reversals quickly moved the adaptive track into the target region for masked threshold. After the fourth reversal, step size was reduced, typically to one-fourth of the initial step size and remained constant for all remaining trials. Trials continued until a total of 12 reversals occurred. The mean of the final eight reversals was taken as the masked threshold.

Masked thresholds were determined in this manner for maskers on electrodes surrounding and including each probe electrode. Testing began with the masker on the probe electrode and proceeded to sequentially more apical or more basal electrodes. The order of testing electrodes (apical-direction-first versus basal-direction-first) was alternated on consecutive retests. Retests continued in the initial and subsequent test sessions until three or more masked thresholds were obtained for each masker electrode. Each point on the *fm*STC was based on the average of three to five forward-masked thresholds. Testing concentrated on one probe electrode at a time. Usually, the middle electrode was tested first. Then either the apical or the basal electrode was tested next.

4. Curve-fitting procedures

To quantify spatial tuning characteristics, each *fm*STC was fitted with two logarithmic functions (log μA vs mm), one on the apical side and one on the basal side (Nelson and Donaldson, 2002; Nelson *et al.*, 2008). Those fits are indicated by the heavy solid curves in the tuning curve plots shown below. Only the steepest portion of each side was included in the least-squares fits. Typically, the fitted function included three or more masked thresholds and accounted for more than 90% of the variance ($R^2 > 0.90$). However, in cases of extremely steep slopes or when the tested electrodes had larger physical separations, only two masked thresholds were included. The fitted slopes are expressed in units of decibels per millimeter to reflect a logarithmic decay in masker current with distance in mm (Black *et al.*, 1983). The spatial bandwidth of the *fm*STC was calculated as the distance (in mm) between the apical and basal fitted slopes at an amplitude 1 dB above the minimum masker level at the tip of the tuning curve.

C. Speech testing procedures

Subjects were assessed with several different measures of speech recognition, including sentence recognition in quiet and in noise and vowel and consonant identification in quiet. Speech testing was conducted at regular intervals throughout the period of time required to collect the *fm*STC data, thus the subjects were quite familiar with the speech testing procedures. Sentence recognition testing was performed using IEEE sentences (IEEE, 1969) spoken by 10 talkers. Each sentence contained five keywords. Subjects verbally repeated each sentence after presentation, and the tester recorded the number of correct keywords. Vowel testing utilized 11 vowels in an h/V/d context (Hillenbrand *et al.*, 1995) spoken by six male talkers. Consonant materials consisted of 19 a/C/a consonants (Shannon *et al.*, 1999) spoken by five male talkers. Both vowel and consonant testing were performed in a closed-set task; subjects identified each vowel or consonant by selecting the appropriate token from a list on a computer screen.

Speech-shaped background noise was generated to match the long-term average spectrum of the sentence materials. The speech and noise were equated in terms of average rms level and mixed to produce a signal-to-noise ratio (SNR) of +10 dB.

Speech recognition testing was conducted in a sound-treated booth. All speech materials were presented at 60 dBA. Subjects used their own speech processors for speech recognition testing with each individual's processor set at their typical use settings; programs optimized for noise reduction were not used. The speech stimuli were presented through either one or two speakers placed 1 m in front of the subject, at 0° azimuth when a single loudspeaker was used, or at 45° azimuth when a pair of loudspeakers was used. For sentence recognition, ten 10-sentence lists were presented in quiet and in noise, with a total of 500 keywords for each condition.

Vowel tokens were presented in the sound field as described in the preceding text. The 11 vowels were presented in 66-item blocks (six presentations of each vowel per block), following a 33-item practice run. Feedback was provided during the practice run but not during the test trials. The average of five blocks was used to calculate percent correct scores with the requirement that all three scores fall within a 10% performance range so that each score was based on 30 presentations of each vowel.

Consonant testing was conducted in the same manner as the vowel testing described in the preceding text with the exception of the number of test tokens. The 19 consonants were presented in 95-item blocks (five presentations of each consonant per block) with a single practice run preceding testing.

Speech recognition performance in quiet and in noise for each subject was compared to various STC parameters to investigate whether measures of spatial tuning were predictive of speech recognition ability. Near the conclusion of the *fm*STC data collection, a second test of vowel identification in quiet and in noise was performed with the same subjects as part of another study. Methods were similar to those described

in the preceding text with the exception that a presentation level of 65 dBA was used, and vowel recognition in steady-state, speech-shaped noise, was measured at a number of SNRs (+20, +15, and +10 dB). To more rigorously explore the relationships between STCs and the perception of specific spectral cues in speech, sequential information analysis (SINFA) was performed on that second set of vowel identification data (Miller and Nicely, 1955).

III. RESULTS AND DISCUSSION

A. Individual differences among *fm*STCs

A wide range of tuning curve shapes were observed within and across subjects; these individual differences will be described in the present section. In later sections, we will describe group trends in the data related to level effects and the effect of electrode region.

Figure 1 shows *fm*STCs obtained from each of the five Advanced Bionics C-I implant users; the *fm*STCs varied noticeably across subjects. In each row of panels, *fm*STCs from the apical, middle, and basal electrode regions are shown in separate panels from left (apical) to right (basal). Two subjects (C03, C16) yielded fairly sharp tuning in all three regions of the electrode array; two subjects (C18, C23) exhibited better tuning on the basal electrode than on the apical or middle electrode, and one subject (C05) exhibited rather broad tuning in all three electrode regions with exceptionally broad tuning on the middle electrode. One subject (C18), who exhibited exceptionally poor tuning on the apical electrode (Fig. 1J) and sharper tuning on the middle and basal electrodes (Figs. 1K and 1L, respectively), also demonstrated higher absolute thresholds (THSm and THSp) in the region of the apical probe electrode than in the regions of the middle and basal probe electrodes. This could be interpreted to mean that most of the excitation on the apical electrode was due to excitation of neural elements in the middle or basal region of the cochlea (near rEL11), where sensitivity was better and tuning was rather sharp (Fig. 1L).

With respect to subject C18, one might speculate that there were non-functioning fibers in the apical region similar to the "dead regions" associated with mistuned forward-masking psychophysical tuning curves in acoustic hearing (Turner *et al.*, 1983; Kluk and Moore, 2006). However, there are a host of other anatomical and physiological factors that can affect the shapes of spatial tuning curves in electric hearing. These include patterns of neural survival along the length of the cochlea, axonal vs dendritic excitation, local impedance of cochlear tissues and aberrant current pathways due to ossification as well as electrode placement (or misplacement). Post-surgical temporal bone x-rays and appropriate spatial reconstruction of electrode position (Seldon, 1991; Marsh *et al.*, 1993; Wang *et al.*, 1996; Ketten *et al.*, 1998; Skinner *et al.*, 2002) could help resolve potential issues related to electrode placement; however, such data were not available for our subjects. Thus it is not possible to know with certainty which anatomical and physiological factors might underlie specific observations of mistuning in our data.

For this group of Advanced Bionics users, stimulated in monopolar mode, the average *fm*STC slope was 1.07 dB/mm and the average bandwidth was 4.37 mm (collapsed across probe level and electrode region). There were a few instances of sharper tuning at the highest probe level (e.g., Figs. 1H and 1I), reminiscent of acoustic tuning curves obtained using high-level probes. In acoustic hearing, high-level probes are presumed to excite broad regions of the cochlea, thus requiring progressively higher-level maskers to mask the spread of excitation with increasing probe level (O'Loughlin and Moore, 1981), often referred to as "off-frequency listening." Similarly, higher-level electric probe stimuli will lead to a broader region of probe excitation, thereby requiring higher-level maskers to overcome the spread of probe excitation on the opposite side of the tuning curve ("off-place listening"). Visual inspection of the tuning curves in Fig. 1 does not suggest consistent differences in the tuning curve shapes for apical or basal probe electrodes as compared to middle electrodes.

Figure 2 shows *fm*STCs obtained from each of five Advanced Bionics C-II implant users. These *fm*STCs were also obtained using a monopolar probe and a monopolar masker. The *fm*STCs from C-II users were generally sharper and more consistent among users than those obtained from C-I users. Some subjects (e.g., D08) exhibited steeper tuning curves in the basal region, while others (e.g., D02) exhibited steeper tuning in the apical region. In addition, there were several examples of "mistuning." For two subjects (D08, D19), *fm*STCs on the middle electrode exhibited "bent tails." In both cases, there were well-shaped tuning curves surrounding the middle electrode, but for the most apical two or three electrodes, low-level maskers easily masked a probe stimulus in the middle of the electrode array. This suggests that there was some atypical current flow from apical electrodes to fibers near the middle of the electrode array.

For this group of subjects, stimulated in a monopolar mode, the average *fm*STC slope was 1.94 dB/mm (81% steeper than C-I) and the average bandwidth was 2.94 mm (67% of the average C-I bandwidth). Generally, the shapes of the *fm*STCs were consistent across probe levels, with a few instances of sharper tuning at the highest probe level (e.g., Fig. 2K). Visual inspection of the tuning curves did not reveal any consistent differences in tuning curve shapes across electrode regions.

Figure 3 shows the *fm*STCs obtained from five Nucleus N-22 users, using bipolar stimulation. They were generally sharper than those obtained from Advanced Bionics C-I and C-II users using monopolar stimulation but demonstrated a number of unique patterns. There were a few examples of very localized tuning with "extended tails," where a tuning curve could be fitted using a few neighboring masker levels on electrodes just above and below the probe electrode, but one side of a tuning curve was quite extended, i.e., low-level stimulation on many remote electrodes would effectively mask the probe electrode. This can be seen for subject N14 [Fig. 3(D)], where the basal tails of tuning curves extended across the entire electrode array. Essentially for probe stimuli on rEL06, the probe was easily masked by low-level stimulation on any of the more basal electrodes (rEL08-rEL22). A similar phenomenon was seen in subject N28, who exhibited extended basal tails on the apical tuning curve

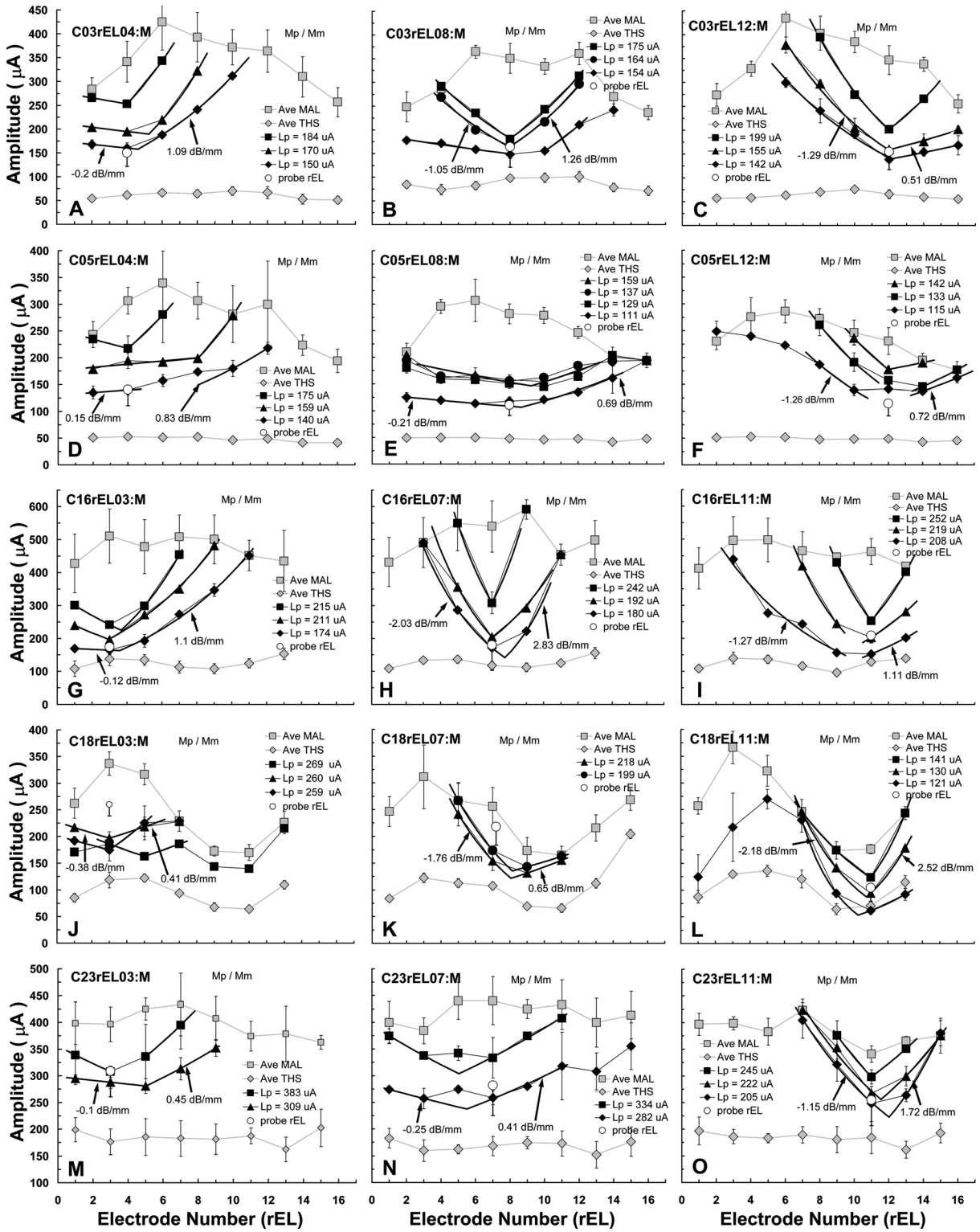

FIG. 1. *fm*STCs obtained from Advanced Bionics C-I implant users. Each graph in a panel shows *fm*STCs obtained at multiple probe levels on one specific electrode. Each row of graphs shows *fm*STCs from a single subject: the left graph is for an apical electrode, the middle graph is for a middle electrode, and the right graph is for a basal electrode. The heading in each panel specifies the subject [e.g., C03 in Fig. 1(A)], the probe electrode pair (rEL04:M, with M for a monopolar reference), and the electrode configuration of the probe and the masker (MPp/MPm, for monopolar probe and monopolar masker) used to generate the *fm*STC. The *x* axis shows electrode number with apical electrodes to the left and basal electrodes to the right. The *y* axis shows stimulus amplitude in μA. The horizontal position of the open circle in each panel corresponds to the active probe electrode; the vertical level of that symbol indicates the probe level (in μA) used to obtain the lowest level *fm*STC. The level of the horizontal bar below the probe symbol indicates the absolute threshold of the probe (THSp). Spatial tuning curves were fitted with apical and basal slopes, shown by the solid lines. Maximum acceptable loudness levels and 3IFC absolute thresholds are shown by the gray symbols. Forward-masked thresholds comprising the *fm*STC are represented by the black symbols, with the error bars indicating 1 standard deviation above and below the mean of at least three threshold measurements. The symbol legend entry indicates the level of the probe used to obtain the thresholds for a specific *fm*STC (e.g., Lp = 150 μA). Forward-masked masker-level thresholds were determined for all activated electrodes in a given electrode array; however, for clarity, thresholds that reached the MALm on a particular masker electrode are not plotted. Average values of MALm and THSm are shown by the gray squares across the top of the graph and the gray diamonds across the bottom of the graph, respectively.

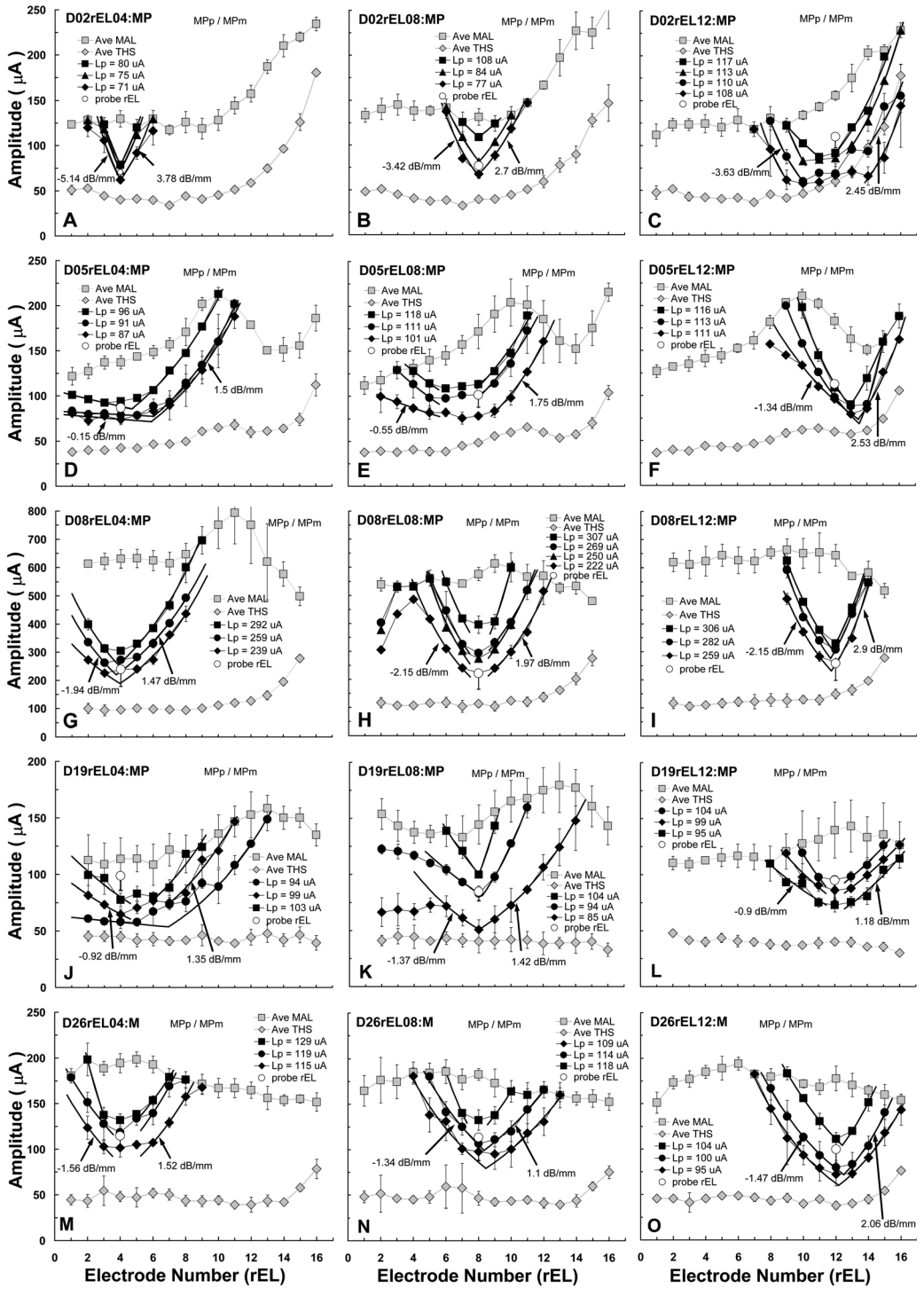

FIG. 2. *fm*STCs obtained from Advanced Bionics C-II implant users. Legend as in Fig. 1.

[Fig. 3(G)] as well as extended apical tails on the basal tuning curve [Fig. 3(I)]. Although some local tuning-curve parameters could be measured on these electrodes, the extended tails raise questions about the effectiveness of that local tuning. Extended tails were also seen in subject N34 but only for the lowest level probe stimulus on rEL05 and rEL10 [Figs. 3(M) and 3(N)]; tuning was well defined on both electrodes for the higher-level probe stimuli. In these subjects with extended tuning-curve tails, there is clearly an interaction between electrical stimulation in the apex and responses in the base and vice versa. This could reflect irregular current pathways due to ossification or misplaced electrodes in the apex or a combination of the two. Whatever the underlying mechanisms, it is clear that these subjects exhibit broad regions of poor spatial selectivity.

A few examples of "mistuning" were also seen among the Nucleus N-22 subjects. For N13, tuning on the basal electrode rEL18 [Fig. 3(C)] was essentially the same as tuning on the middle electrode rEL11 [Fig. 3(B)]. For this subject, there appears to be no viable region of functional fibers in the basal half of the cochlea. Mistuning on rEL17 can also be seen for subject N34 [Fig. 3(O)], where a second

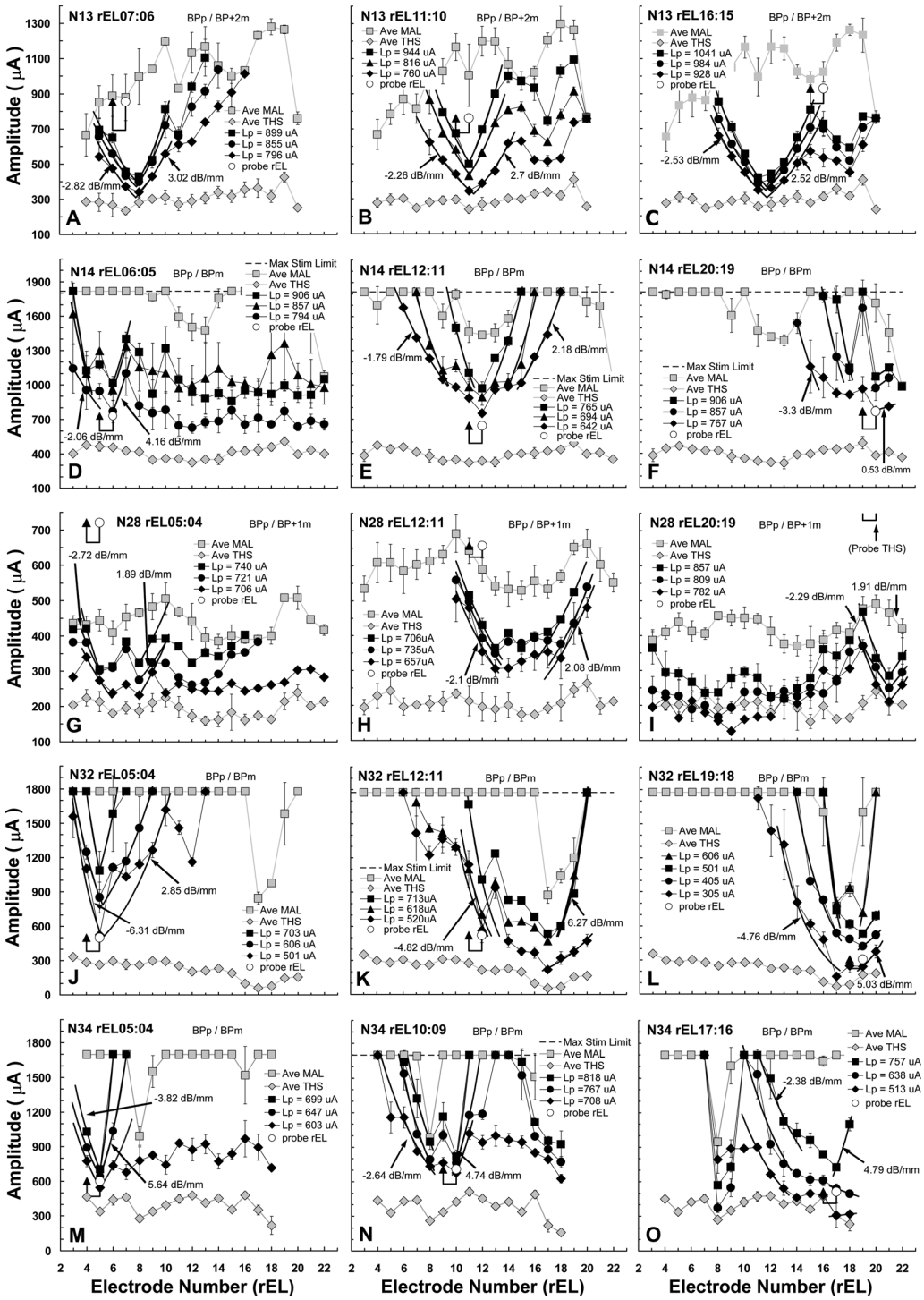

FIG. 3. *fm*STCs obtained from Nucleus N22 implant users. The heading in each panel specifies the subject code [e.g., N13 in Fig. 3(A)], the probe electrode pair (rEL07:08), and the electrode configuration of the probe and the masker (BPp/BP + 2m, for bipolar probe and bipolar + 2 masker) used to generate the *fm*STC. For some subjects, a BP masker was not sufficiently loud to masker the BP probe, therefore the spatial extent between the active and reference electrodes was extended by one or two electrodes (e.g., BP + 2 for N13). The active electrode of the bipolar probe electrode pair is indicated by an open circle connected to an up arrow that indicates the reference electrode of the pair. The solid line connecting the two indicates the absolute threshold for the probe stimulus. The dashed line across the top of some of the graphs indicates the maximum current amplitude that could be generated by a subject's device.

minimum in the basal tuning curve was evident near rEL08-rEL09.

The average slope of *fm*STCs shown in Fig. 3 was 3.6 dB/mm (86% steeper than C-II, 236% steeper than C-I) and the average bandwidth was 1.9 mm (67% of the average C-II bandwidth, and 43% of the average C-I bandwidth). Again, visual inspection of the tuning curves did not reveal any consistent differences in general shape across electrode region. However, there were obvious discontinuities in some individual tuning curves at some probe levels. For example, at the lowest level, N14 exhibited a relatively broad tuning curve on rEL20 [Fig. 3(F)]; at the two higher probe levels, tuning curves were narrower and exhibited a clear central notch. Similarly, N32 [Fig. 3(K)] showed sharper tuning

curves at the higher two probe levels along with notches just basal to the probe tone.

B. Spatial tuning characteristics of the *fm*STC

To quantify spatial tuning characteristics across subjects and probe levels, each *fm*STC was fitted with two logarithmic functions, one on the apical side and one on the basal side. As indicated by the heavy solid curves in the previous figures, only the steepest portions of the tuning curves were included in the least-squares fits. Typically, three or more masked thresholds along the steepest portion of the curves on each side of the probe electrode (not including the probe electrode) were included in a fitted slope, resulting in a regression coefficient (R^2) greater than 0.90. The fitted slopes were expressed in units of decibels per millimeter. The *fm*STC bandwidth was calculated as the distance (in mm) between the apical and basal fitted slopes at a masker level that was 1 dB above the minimum masker level. The *fm*STC "tip" was specified at the midpoint of the bandwidth, and the amount of tip shift ("mistuning") was specified as the distance between the tip place and the probe electrode place (in mm). These metrics for quantifying *fm*STCs focus on the steepest portion of the tuning curve and ignore irregularities that sometimes occur close to the probe electrode; they also ignore irregularities that occur remote from the probe, such as the bent or extended tails described earlier in some subjects.

1. Effects of probe level

To evaluate the effects of probe level on *fm*STC slopes and bandwidths, those parameters were first normalized to the values obtained for the middle of three probe levels (or the highest probe level when only two levels were tested).[1] The resultant slope ratios and bandwidth ratios were then subjected to linear regression analysis [slope ratio or bandwidth ratio vs probe level expressed in percent of dynamic range in microamps (%DRμA)]. Separate regressions were performed for each of the three subject groups at each of the three electrode regions. The results are listed in Table II. Three of the 18 linear regressions (bold type) yielded significant correlation coefficients ($P < 0.05$), but the strength of these correlations was modest (R^2 values between 0.31 and 0.37). None of the remaining regression coefficients were significant. Overall, these findings indicate that *fm*STC shapes were not systematically influenced by probe level at least for probe levels in the range of 10% to 30% DRμA.

To further evaluate possible differences across the three subject groups, the slope ratios and bandwidth ratios were combined across apical, middle, and basal electrode regions and subjected to regression analyses using a power function. The combined slope ratios and width ratios are plotted in Figure 4 as a function of the average probe level in %DRμA along with the power-function fits. The average level of the probe (Ave Lp) shown on the abscissa is based on the average of at least three MALp and THSp measurements obtained over multiple test sessions. In each graph, the relative change in STC slope or STC width is shown as a function of the relative change in probe level. For the C-I subject group, there was a significant trend for bandwidths to decrease with increasing probe level ($R^2 = 0.31$, $P < 0.01$); however, this relationship was driven largely by the unusually wide bandwidths of two subjects (C16 and C03) at the lowest probe levels. None of the other regression coefficients were significant. Thus the power-function analyses were consistent with the linear regression analyses, described in the preceding text, and indicated that probe level had little or no influence on *fm*STC parameters.

TABLE II. Results of regression analyses of level effects in three electrode regions, for subjects with C-I, C-II, and N-22 devices.

STC Parameter (y)	a	b	R^2	F	df	P
Clarion C-I devices (monopolar)						
Slope in dB/mm						
Apical region	1.29	0.75	0.227	3.529	13	0.08
Middle region	0.72	0.89	0.104	1.273	12	0.28
Basal region	0.41	0.90	0.037	0.495	14	0.49
Q1dB Width in mm						
Apical region	−3.24	1.90	0.204	3.066	13	0.11
Middle region	−2.71	1.71	0.121	1.516	12	0.24
Basal region	−1.83	1.34	**0.370**	7.635	14	**0.02**
Clarion C-II devices (monopolar)						
Slope in dB/mm						
Apical region	1.16	0.78	**0.306**	5.719	14	**0.03**
Middle region	−0.77	1.16	0.046	0.630	14	0.44
Basal region	0.34	0.93	0.006	0.083	14	0.78
Q1dB Width in mm						
Apical region	−0.71	1.21	0.047	0.644	14	0.44
Middle region	1.12	0.85	0.054	0.738	14	0.41
Basal region	−2.15	1.38	0.093	1.326	14	0.27
Nucleus N-22 devices (bipolar)						
Slope in dB/mm						
Apical region	1.33	0.88	0.098	1.417	14	0.26
Middle region	1.46	0.73	**0.360**	7.317	14	**0.02**
Basal region	0.44	1.26	0.004	0.049	14	0.83
Q1dB Width in mm						
Apical region	−0.89	1.06	0.061	0.839	14	0.38
Middle region	0.04	0.95	0.0001	0.001	14	0.97
Basal region	−0.05	0.94	0.0002	0.002	14	0.96

Dependent variable (y) is either the slope or width ratio, which are the relative changes in STC slope or STC width as a function of probe level (%DR in μA). Linear regression: $y = ax + b$, x = probe level (%DRuA).

2. Effects of electrode region

Because there was little or no effects of probe level on *fm*STC parameters for any of the three subject groups, tuning curve parameters were collapsed across probe level to examine the effects of electrode region. Figure 5 shows the average parameter values for slope and bandwidth for each subject group and electrode region. Tuning curve slopes are shown in the left-hand panel and tuning curve bandwidths are shown in the right-hand panel.

A two-way (group × electrode) repeated measures analysis of variance (ANOVA) was performed to confirm the observed differences in *fm*STC slopes across subject groups and electrode locations. There was a significant main effect of group ($F^{2,12} = 12.45$, $p = 0.001$), but no significant main

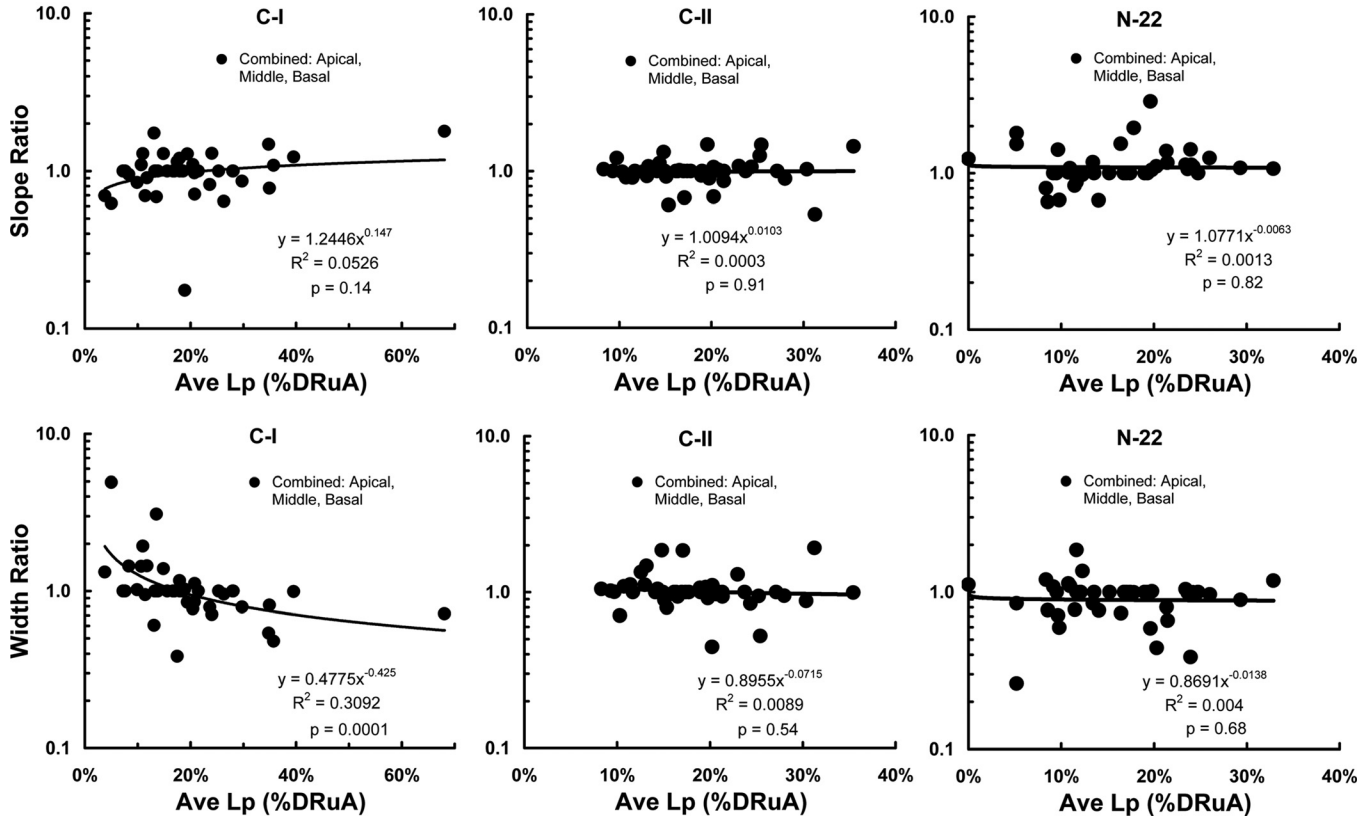

FIG. 4. Level effects: slope ratios and width ratios of *fm*STCs as a function of probe level expressed as %DR in microamps (μA). Ratios are defined in the footnote.

effect of electrode [$F(2,12) = 0.50$, $P = 0.612$] or group $\times$ electrode interaction [$F(4,12) = 1.62$, $P = 0.200$]. *Post hoc* Holm-Sidak pairwise comparisons indicated that slopes were significantly greater for N-22 subjects than for C-I subjects ($t = 4.91$, $P = 0.001$) or C-II subjects ($t = 3.20$, $P = 0.015$); slopes for C-I and C-II subjects were not significantly different from each other ($t = 1.71$, $P = 0.112$).

A similar two-way ANOVA was performed on the *fm*STC bandwidths. There was a significant main effect of group [$F(2,12) = 6.79$, $P = 0.011$], but no significant main effect of electrode [$F(2,12) = 2.16$, $P = 0.136$] or group $\times$ electrode interaction [$F(4,12) = 1.76$, $P = 0.168$). *Post hoc* Holm- Sidak pairwise comparisons indicated that bandwidths were significantly smaller for N-22 subjects than for C-I subjects ($t = 3.67$, $P = 0.010$) but were not significantly different for N-22 subjects than for C-II subjects ($t = 1.54$, $P = 0.148$). Bandwidths for C-I and CII subjects were not significantly different from each other ($t = 1.71$, $P = 0.112$).

In summary, the statistical analyses indicate that there were no systematic differences in *fm*STC slopes or bandwidths across electrode regions for any of the subject groups. From this we can conclude that tuning curves obtained on apical, middle, and basal electrodes have the same general shape. This conclusion holds for the monopolar electrode configurations in C-I and C-II users and bipolar electrode configurations in N-22 users.

The steeper STC slopes and narrower bandwidths for the N-22 subjects are consistent with some of the expected

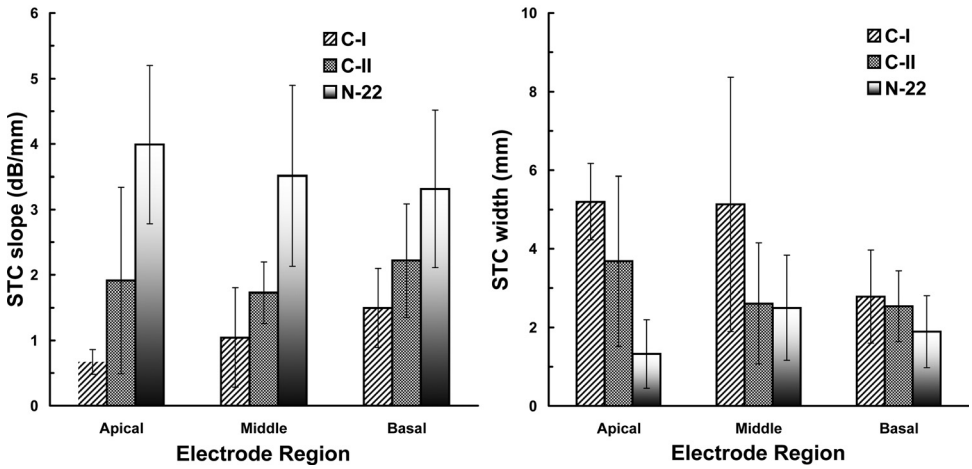

FIG. 5. Electrode-region effects: Average slopes of *fm*STCs and widths of *fm*STCs expressed in mm. Error bars indicate one standard deviation each side of the mean.

effects of BP stimulation for the N-22 subjects compared with MP stimulation for the C-I and C-II subjects (Finley *et al.*, 1990; Liang *et al.*, 1999; Boex *et al.*, 2003; Bierer, 2007; Snyder *et al.*, 2008; Landsberger and Sirinivasan, 2009; Bierer and Faulkner, 2010). However, it should be noted that the current research was not intended to evaluate electrode configuration *per se* (MP vs BP); that endeavor requires a within-subjects research design. One study that used a within-subjects design did not find sharper forward masking patterns with a BP compared to a MP electrode configuration when overall level differences were taken into account (Kwon and van den Honert, 2006). Unfortunately, in that study, both masker and probe were presented in the same mode as in the present study. Ideally, one would like to know whether a broader *fm*STC is due to the stimulation of a broader population of surviving nerve fibers by the probe or to a more gradual spread of current throughout the cochlea by the masker. Therefore a valid test of the effects of BP and MP configurations with *fm*STCs requires that the configuration of the probe is held constant, while electrode configuration of the masker is varied and vice versa. For example, the shape of an *fm*STC might be broader with a BP probe, relative to an MP probe, simply due to the increased amplitude required to reach absolute probe threshold with BP stimulation (Bierer and Faulkner, 2010). In that case, the increased probe amplitude results in a broader spread of probe current to recruit a sufficient population of surviving nerve fibers to reach absolute threshold. Then higher level maskers are required to mask that population and the slopes of the *fm*STCs are more gradual. Alternatively, the shape of an *fm*STC might be broader with an MP masker because the spread of current along the cochlear duct is more gradual with an MP stimulus than with a BP stimulus (Black *et al.*, 1983). A recent comprehensive review of electrode configuration effects (Bonham and Litvak, 2008) suggests that additional research is required to understand how electrode configuration may influence spatial selectivity in individual cochlear implant users.

C. Frequency tuning characteristics of the *fm*STC

To compare spatial tuning in electric hearing with frequency tuning in acoustic hearing, spatial locations along the electrode array were converted into the frequencies associated with each location in acoustic hearing using Greenwood's (1960) frequency-place map for the human cochlea. Electrode locations were estimated using surgeons' reports of the insertion depths of individual subject's electrode arrays. A cochlear length of 35 mm was assumed for all subjects.

Figure 6 shows *fm*STCs from apical, middle, and basal electrodes in one subject (D08) that have been converted to a "Greenwood" frequency scale. Each side of the tuning curve is well fit with a linear function in units of decibels/octave. The bandwidth (in Hz) was computed between the apical and basal slopes at a masker level 1 dB above the minimum masker level. For comparisons with frequency tuning in acoustic hearing, each *fm*STC bandwidth was converted to a "Q-factor," defined as the ratio between the characteristic frequency associated with the probe electrode and the 1-dB *fm*STC bandwidth. Because dynamic ranges are approximately 10 times larger in acoustic hearing than in electric hearing (Nelson *et al.*, 2008), bandwidth measurements taken 1 dB above the tip of the spatial tuning curve are comparable to bandwidth measurements taken at the typical level used in acoustic hearing, i.e., 10 dB above the tip of the frequency tuning curve. The apparent sharper tuning curves for the basal electrode (right-hand panel) than the apical electrode (left-hand panel) in the example shown in Fig. 6 are not the product of transforming electrode distance to a place frequency scale, they are a characteristic of this example subject. The analyses in the following text will show that, on average, transformed-frequency tuning curve shapes did not differ significantly across electrode regions.

Figure 7 shows the slopes and bandwidths of *fm*STCs at each cochlear region, expressed in terms of Greenwood frequency. As seen in the left-hand graph, the mean slope values for the N-22 users varied between 16 and 17 dB/octave

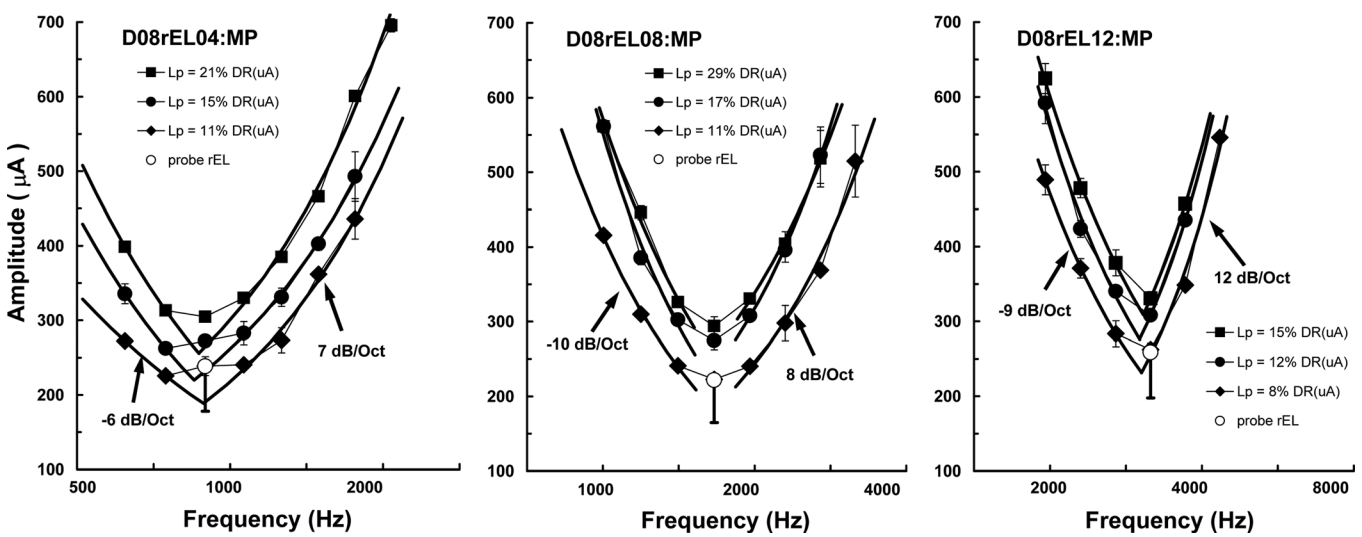

FIG. 6. Spatial tuning curves plotted in terms of frequency calculated from Greenwood's (1960) place-frequency map.

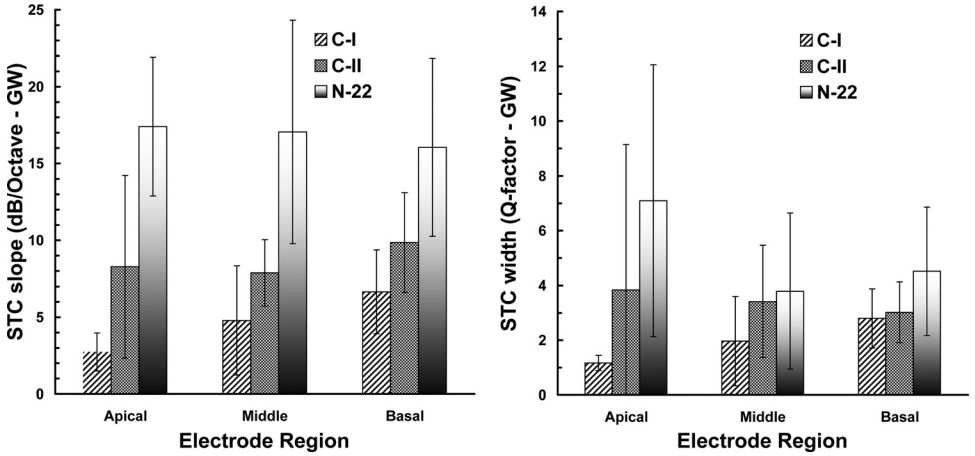

FIG. 7. Electrode-region effects: Slopes of *fm*STCs and widths of *fm*STCs expressed in terms of frequency calculated from Greenwood's (1960) place-frequency map. GW, Greenwood frequencies. Error bars indicate one standard deviation each side of the mean.

across electrode regions with an average slope of 16.8 dB/octave. Mean slope values for the C-II users varied between 8 and 10 dB/octave across electrode regions with an average slope of 8.7 dB/octave. Mean slope values for the C-I users varied between 2.7 and 6.6 dB/octave across electrode regions with an average slope value of 4.7 dB/octave.

A two-way (group × electrode) repeated measures ANOVA performed on frequency slopes indicate a significant main effect of group [$F(2,12) = 15.22$, $P < 0.001$], no main effect of electrode [$F(2,12) = 0.67$, $P = 0.517$], and no group × electrode interaction [$F(4,12) = 0.89$, $P = 0.485$]. *Post hoc* Holm-Sidak pairwise comparisons indicated that frequency slopes were significantly greater for N- 22 subjects than for C-I subjects ($t = 5.41$, $P = 0.001$) or C-II subjects ($t = 3.64$, $P = 0.007$), but that frequency slopes did not differ significantly for C-I and C-II subjects ($t = 1.76$, $P = 0.103$).

On average, the frequency slopes obtained from the N-22 users, who were stimulated using a bipolar electrode configuration, were nearly twice as steep as those obtained from C-II users and more than three times steeper than those obtained form C-I users, who were stimulated using a monopolar configuration.

The STC bandwidths are shown in the right-hand panel of Fig. 7, expressed here as frequency Q-factors, as in acoustic hearing. The frequency Q-factor is the center frequency of the tuning curve divided by its bandwidth in hertz (the higher the Q factor the narrower the bandwidth). The mean Q-factor for the N-22 users varied between 3.8 and 7.1 across electrode regions with an average Q-factor of 5.1. Mean slope values for the C-II users varied between 3.0 and 3.8 with an average Q-factor of 3.42. Mean slope values for the C-I users varied between 1.2 and 2.8 with an average Q-factor of 1.98.

A two-way (group × electrode) repeated measures ANOVA performed on frequency Q-factors indicates a significant main effect of group [$F(2,12) = 4.69$, $P < 0.031$], no main effect of electrode [$F(2,12) = 0.41$, $P = 0.662$], and no group × electrode interaction [$F(4,12) = 0.90$, $P = 0.477$]. *Post hoc* Holm-Sidak pairwise comparisons indicated that frequency Q-factors were significantly greater for N-22 subjects than for C-I subjects ($t = 3.06$, $P = 0.029$) but not different from C-II subjects ($t = 1.65$, $P = 0.231$); frequency Q-factors did not differ significantly for C-I and C-II subjects ($t = 1.40$, $P = 0.187$). However, the significantly greater Q-factors for the N-22 subjects relative to C-I subjects was due to differences on the apical electrode alone ($t = 3.23$, $P = 0.008$).

On average, the tuning-curve bandwidths obtained from the N-22 users stimulated using a bipolar electrode configuration were more than 2.5 times narrower than those obtained from C-I users stimulated using a monopolar configuration; this was primarily due to differences on the apical electrode.

D. Comparisons with tuning in acoustic hearing

In our earlier work (Nelson *et al.*, 2008), we compared *fm*STC-based measures of spatial tuning in cochlear implant listeners with previously reported measures of frequency tuning in normal-hearing and hearing-impaired acoustic listeners obtained from forward-masked psychophysical tuning curves (*fm*PTCs). Specifically, parameters from the *fm*STCs obtained on a middle electrode were compared to parameters from *fm*PTCs obtained at 1 000 Hz in normal-hearing listeners and listeners with sensorineural hearing loss (Nelson, 1991). The acoustic tuning curves were obtained with a forward-masking procedure similar to that used in the present study. The *fm*STC slopes measured in cochlear implant users were similar to *fm*PTC slopes measured in listeners with moderate cochlear hearing loss and to tail slopes of *fm*PTCs in normal-hearing listeners. In acoustic hearing, *fm*PTC tail slopes reflect the broad cochlear tuning associated with passive cochlear mechanics and contrast with the sharper frequency selectivity imposed on that broader tuning by a healthy outer hair cell system. In electric hearing, *fm*STC slopes can only reflect current spread throughout cochlear tissues.

Unfortunately, a database of tuning-curve slopes like that published for 1000-Hz *fm*PTCs (Nelson, 1991) does not exist for other acoustic frequencies. Therefore it was not possible to compare *fm*STC slopes for apical and basal electrodes with *fm*PTC slopes from comparable frequency regions in acoustic hearing. However, estimates of frequency-selectivity *bandwidths* across the frequency spectrum do exist for normal-hearing listeners. One study examined bandwidths at

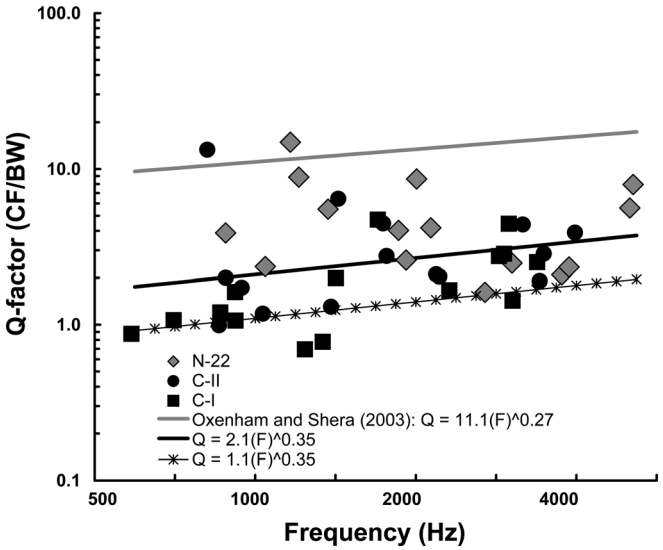

FIG. 8. Comparisons of Q-factor estimates in electric and acoustic hearing. Black squares and circles show Q-factors (characteristic frequency/bandwidth) obtained from C-I and C-II users with monopolar configurations, respectively. Gray diamond symbols show Q-factors obtained from N22 users with bipolar configurations. The gray upper line shows Q-factor estimates obtained from "equivalent-rectangular-bandwidth" measures (Qerb) by Oxenham and Shera (2003) for acoustic hearing using forward masking procedures. The black lower line is the best-fit power function to the Q-factors from all of the cochlear implant users. The asterisked line shows the predicted Q-factors for acoustic listeners with cochlear hearing loss, calculated from *fm*PTC data published by Nelson (1991).

different frequency regions using simultaneous masking procedures (Glasberg and Moore, 1990), while others utilized forward masking procedures (Moore, 1978; Shera *et al.*, 2002; Oxenham and Shera, 2003) that yielded slightly narrower estimates. Such bandwidth estimates are commonly reported as Q-factors, where the Q-factor is defined as the characteristic frequency divided by the bandwidth.

Figure 8 shows Q-factors calculated from the three groups of cochlear implant users in the present study along with Q-factors from normal-hearing acoustic listeners. The solid black symbols show Q-factors for Advanced Bionics C-I and C-II cochlear-implant users stimulated in a monopolar electrode configuration. Q-factors for C-I users ranged from 0.87 to 4.7 with mean values of 1.2, 2.0, and 2.8 on apical, middle, and basal electrodes, respectively. Q-factors for C-II users ranged from 1.0 to 13.3 with mean values of 3.8, 3.4, and 3.0 on apical, middle, and basal electrodes, respectively. The statistics reported in the preceding text indicated there were no significant differences in Q-factors for C-I and C-II subjects. Q-factors for the Nucleus N-22 users, stimulated with bipolar electrode configurations, are shown in Fig. 8 by the gray diamond symbols. They ranged from 1.6 to 14.9 with mean values of 7.1, 3.8, and 4.5 on apical, middle, and basal electrodes, respectively. The statistics reported in the preceding text indicated that the N-22 users, with bipolar electrode configurations, exhibited significantly larger Q-factors (narrower bandwidths) than the C-I users, with monopolar electrode configurations, but only for apical electrodes. That finding is seen quite clearly in Fig. 8 where the larger Q-factors for the N-22 subjects occur at the lower frequencies. At the higher frequencies the Q-factors for the three groups overlap.

Oxenham and Shera (2003) examined frequency-selectivity bandwidths in normal-hearing acoustic listeners across a wide range of acoustic frequencies. Using notched noise masking data, they found that for low-level acoustic stimuli, the Q-factor for acoustic hearing is well defined by a power function of acoustic frequency given by $Q = 11.1(F)$^0.27, where F is the test frequency in kilohertz. This function is represented in Fig. 8 by the upper gray line labeled Oxenham and Shera (2003). For comparison purposes, the Q-factors for cochlear implant users in the present study were fit with a power function of frequency. This function is shown in Fig. 8 by the lower black line, defined by $Q = 2.1(F)$^0.35, $R^2 = 0.15$. Note that the slope of the electric function (0.35) is only slightly steeper than the slope of the acoustic function (0.27), indicating that there is a trend in the electric data toward increasing Q-factors with frequency, similar to that in the acoustic data. In contrast, the intercept of the electric function (at 1 kHz) of 2.1 is considerably smaller ($\sim 1/5$) than the intercept of the acoustic function of 11.1. This suggests that frequency bandwidths in electric hearing are about five times wider than frequency bandwidths observed in normal acoustic hearing. Note, however, that this comparison is based on low-level stimuli in acoustic hearing, where the active tuning mechanisms of outer hair cells in the normal cochlea contribute strongly to frequency tuning (Ruggero, 1992). At higher sound levels frequency Q-factors in acoustic hearing are reduced considerably (Nelson, 1991).

Because electric hearing does not involve contributions by active cochlear tuning mechanisms, a more appropriate comparison should, perhaps, involve measures of frequency bandwidths in acoustic hearing that are minimally influenced by those mechanisms. Such measures have been reported (Nelson, 1991) for a group of 10 listeners with moderate cochlear hearing loss (41–66 dB HL) at 1 000 Hz. The *fm*PTCs for these listeners, with tip levels between 67 and 82 dB SPL, exhibited Q-factors between 0.5 and 2.1 with an average Q-factor of 1.1. Assuming that the change in Q-factor with frequency is similar to that for the present cochlear implant subjects (exponent = 0.35), then the predicted Q-factors for moderate cochlear hearing loss (without active tuning mechanisms) are represented by the line connecting the asterisks in Fig. 8 [$Q = 1.1(F)$^0.35]. According to this prediction, cochlear implant users in the present study demonstrated Q-factors that were slightly better than those for acoustic listeners with moderate cochlear hearing loss. However, it should be noted that the bandwidths of *fm*PTCs for the hearing impaired listeners were measured 10 dB above their tips. Because hearing loss reduced the effective dynamic range from approximately 100 to 50 dB, this level was closer to 20% of the dynamic range than 10% of the dynamic range as used with normal-hearing listeners and cochlear-implant listeners. Narrower bandwidths (and larger Q-factors) would be expected if a similar, 10% dynamic range criterion was used for the hearing-impaired listeners; in that case, the Q-factors from the cochlear-implant users would fall within the same range of values as the hearing-impaired listeners.

This reasoning leads us to conclude that the spatial selectivity of cochlear implant users is comparable to the frequency selectivity of acoustic listeners who lack functional outer hair cells (Dallos and Harris, 1978; Liberman and Dodds, 1984). However, this conclusion is based on estimates of spatial tuning (*fm*STC parameters) that were obtained using direct stimulation of the implanted electrodes (i.e., bypassing the speech processor). While these measures of spatial selectivity reflect current spread in the cochlea, irregular patterns of neural survival and changes in central auditory tuning, they do *not* account for additional factors that might influence spatial resolution when acoustic stimuli are presented through a speech processor, e.g., the limited number of stimulation sites (electrodes) available in traditional implant systems, the broad fixed-frequency bandwidths of analysis filters used in implant speech processors, the instantaneous nonlinear amplitude mapping, and the automatic gain control that precedes the mapping. Thus while basic measures of tonotopic selectivity appear to be similar, on average, for implant users and for acoustic listeners with substantial outer hair cell damage, it does not necessarily follow that the two types of listeners possess similar levels of spectral resolution for complex acoustic stimuli delivered through a speech processor.

E. Comparisons with speech recognition

Speech performance in quiet is reported in Table I as percentage correct for consonant and vowel identification and recognition of key words in sentences in quiet and in noise (+10 dB SNR); these results were the scores achieved on the final speech test administered during the *fm*STC data collection period. Performance in quiet for consonant identification ranged from 27.2% to 82.7% and for vowel recognition from 40% to 92.7%. Percentage correct for key words on sentence materials ranged from 3.6% to 76% in quiet and from 0.4% to 48.2% in noise with a +10 dB SNR.

Performance in quiet and in noise on each of the original speech measures was compared with various STC parameters, including apical, middle, and basal STC bandwidths and slopes, the average of the three BW and slope measures for each subject, a weighted average, as well as the "best" and "worst" BW and slope measures. The weighted average gave the middle electrode parameter twice the weight of the corresponding apical and basal electrode parameters in an attempt to reflect the greater importance of information in the spectral region of 1500-2000 Hz for intelligibility of speech (French and Steinberg, 1947; Boothroyd, 1967), which corresponds roughly to the inferred frequency location of the middle STC probe electrode. No significant correlations ($P < 0.05$) were found between any of the factors examined.

SINFA analysis of the second vowel data set focused on relative transmitted information (RTI) for the first and second vowel formant (F1 and F2) features. In particular, parameters reflecting spatial resolution of middle electrodes were thought to be most likely to show a relationship with RTI for the F2 feature because the frequency range of F2 for these materials (933-2316 Hz, with an average of 1554 Hz) is closer to the center frequency of the filter for the middle probe electrode than apical or basal electrodes. While no significant correlations were found after corrections were applied to α for multiple comparisons, a trend can be seen in Fig. 9 between transmitted information for the vowel F2 feature in noise (+20 dB SNR) and both the STC slope (left-hand panel) as well as the STC bandwidth (right-hand panel) parameters for the middle electrode.

In summary, there were no strong relationships between measures of speech perception (sentence, vowel, or consonant identification) and spatial tuning parameters. Even when the reception of specific spectral cues was examined (e.g., first two formant frequencies of vowels), where spatial tuning might be expected to play a more direct role, no significant relationships emerged. These findings are consistent with other published reports that also failed to show significant relationships between measures of spatial selectivity and speech recognition (Zwolan *et al.*, 1997; Cohen *et al.*, 2003; Hughes and Stille, 2009). On the other hand, several previous studies have demonstrated significant relationships between speech perception and measures of spectral resolution determined by pitch-ranking experiments (Donaldson and Nelson, 2000; Donaldson *et al.*, 2011).

One might predict that sharper *fm*STCs (suggesting better spectral resolution) would result in excitation patterns in response to speech stimuli that better preserve spectral contrast in the original acoustic waveform, thereby producing

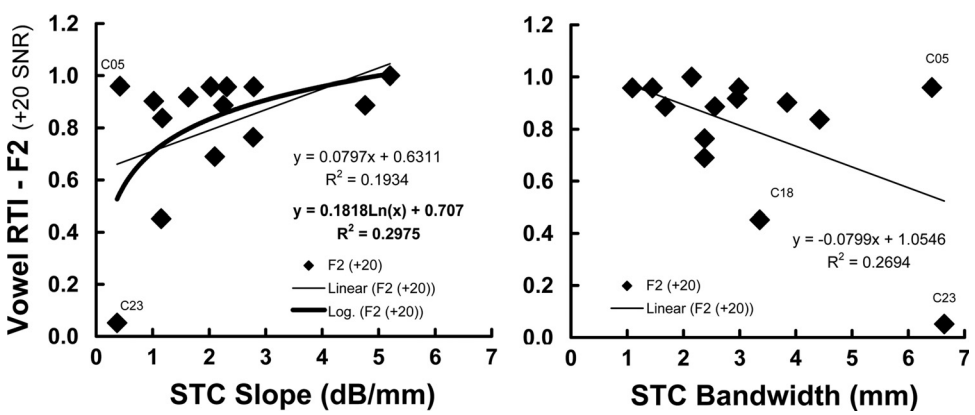

FIG. 9. Rate of transmitted information (RTI) for feature F2 in vowel identification at an SNR of +20 dB as a function of STC slope (dB/mm) on the middle electrode (left panel) and as a function of weighted average BW (mm) on the middle electrode (right panel).

better speech recognition. However, when speech is presented through the speech processor, other factors can influence not only spectral contrast but also general spectral patterns in the electrical stimulus (e.g., band-pass filter frequency allocations and filter slopes, amplitude compression functions, and pulse rate insofar as it impacts loudness growth). Thus the lack of a relationship between *fm*STC parameters and speech recognition may be explained, at least in part, by the differences in stimulus presentation, i.e., direct stimulation in the *fm*STC experiment, versus stimulation through an individual subject's speech processor for the speech experiments.

In the present study, speech recognition measures included sentences as well as phonemes. It is not surprising that measures of spatial selectivity were not significantly correlated with sentence recognition scores because sentence materials contain temporal cues and contextual cues that subjects may have been able to utilize in the absence of good spectral information. Phonemic cues that are more purely coded in the spectral domain (e.g., transmitted information for vowel F1 and F2 features) should provide a more realistic indication of the role of spatial selectivity in speech recognition. In the present study, a trend was observed for *fm*STCs to predict information transmission related to vowel F2 frequency; however, this trend did not reach significance.

V. SUMMARY AND CONCLUSIONS

*fm*STCs were obtained from each of five Advanced Bionics C-I and five Advanced Bionics C-II cochlear implant users, stimulated in a monopolar electrode configuration, and from each of five Nucleus N-22 cochlear implant users stimulated in a bipolar electrode configuration. In each subject, *fm*STCs were obtained at several probe levels for each of three (apical, middle, and basal) electrodes. Slopes and bandwidths of *fm*STCs were compared across probe levels, subject groups and cochlear regions. Spatial tuning bandwidths were compared with published estimates of frequency selectivity in normal hearing and hearing-impaired acoustic listeners. In addition, spatial tuning parameters were compared with speech recognition measures obtained in quiet and in noise. Analyses led to the following key findings and conclusions:

- The *fm*STCs from apical, middle, and basal electrodes were well characterized by apical and basal slopes (in dB/mm) and by bandwidths (in mm) measured 1 dB above the tuning-curve tip.
- Slopes of *fm*STCs from apical, middle, or basal electrodes were relatively independent of probe level for probe levels between 10% and 30% of the dynamic range of the probe stimulus.
- The *fm*STCs for apical, middle, and basal electrodes had the same general shape. There were no significant effects of electrode region for any of the three subject groups.
- Slopes of *fm*STCs were significantly steeper for subjects stimulated with a bipolar electrode configuration (N-22 users) than for subjects stimulated with a monopolar electrode configuration (C- I and C-II users). This was true for apical, middle, and basal electrodes evaluated separately and when all three electrode regions were combined.
- Bandwidths of *fm*STCs measured 1 dB above the STC tip were not significantly different for bipolar and monopolar subjects when all three electrode regions were combined. However, bandwidths were significantly narrower for bipolar configurations on the apical electrode alone.
- *fm*STCs converted to frequency coordinates, by calculating the frequency corresponding to each electrode using a tonotopic place-frequency function (Greenwood, 1990), yielded slopes of *fm*STCs that were similar to the tail slopes of tuning curves measured in acoustic listeners. Consistent with this, bandwidths of *fm*STCs were similar to bandwidths measured in acoustic listeners at high stimulus levels and in listeners with moderate cochlear hearing loss.
- The average frequency Q-factor in electric hearing is about 1/5 of that reported for normal acoustic hearing at low stimulus levels. Q-factors from cochlear-implant users are within the same range as Q-factors obtained from acoustic listeners with moderate cochlear hearing loss. Thus spatial resolution in electric hearing is similar to the broad tuning in the cochlea that is observed in the absence of active tuning from outer hair cells.
- No robust relationships were identified between measures of speech perception (sentence, vowel, or consonant identification) and spatial tuning parameters. Even when the reception of specific spectral cues was examined (e.g., first two formant frequencies of vowels), where spatial tuning might be expected to play a more important role, no significant relationships emerged.

ACKNOWLEDGMENTS

This work was supported by National Institute on Deafness and Other Communcation Disorders Grant No. R01-DC006699 and by the Lions 5M International Hearing Foundation. Advanced Bionics Corporation provided the research interface and some of the software required for testing Advanced Bionics C-I and C-II subjects. Eric Javel developed the experimental software to control the C-I interface. Andrew Oxenham contributed to the development of experimental software to control the C-II interface. Cochlear Corporation provided Nucleus N-22 subjects' calibration tables. John Van Essen converted Robert Shannon's computer software into the C language and made modifications to that software for testing Nucleus N-22 subjects. The authors extend special thanks to the subjects who devoted many hours of listening to this work.

APPENDIX

For the reader who may be interested in examining the raw data, *fm*STC parameters for each of the 15 subjects are summarized in the following tables. Tables III–V are organized by subject group (Clarion C-I, Clarion C-II, and Nucleus N22 cochlear implant users, respectively).

TABLE III. Spatial tuning curve parameters in Clarion C-I implant users.

Subj ID	rEL	Ave Lp (%DRuA)	STC Slope (dB/mm)	STC width (mm at Q1dB)	Cf (GW Hz)	GW slope (dB/Octave)	GW width Q-factor
C03	4	17.9	0.78	6.42	586	3.45	0.87
	8	17.1	1.02	3.23	1 416	4.67	1.99
	12	20.1	0.99	2.49	2 863	4.67	2.75
C05	4	27.6	0.50	5.05	860	2.62	1.20
	8	15.3	0.42	7.94	1 339	1.88	0.78
	12	19.9	0.82	4.74	3 036	4.49	1.43
C16	3	11.3	0.95	5.01	703	4.30	1.07
	7	16.2	2.25	1.41	1 697	10.42	4.71
	11	9.5	1.62	2.40	2 927	7.66	2.84
C18	3	15.3	0.53	3.80	917	2.30	1.62
	7	14.1	1.15	4.04	2 311	5.30	1.66
	11	19.7	2.32	1.55	2 988	10.98	4.44
C23	3	48.1	0.59	5.72	919	1.01	1.06
	7	28.8	0.37	9.05	1 239	1.63	0.69
	11	26.1	1.73	2.74	3 378	5.46	2.52
Group averages by electrode region:							
Apical	Ave	24.0	0.67	5.20	797	2.74	1.17
	s.d.	14.7	0.19	0.97	147	1.24	0.28
Middle	Ave	18.3	1.04	5.13	1 601	4.78	1.97
	s.d.	6.0	0.76	3.24	432	3.55	1.63
Basal	Ave	19.1	1.50	2.79	3 038	6.65	2.80
	s.d.	6.0	0.60	1.18	201	2.73	1.08

TABLE IV. Spatial tuning curve parameters in Clarion C-II implant users.

Subj ID	rEL	Ave Lp (%DRuA)	STC Slope (dB/mm)	STC Width (mm at Q1dB)	Cf (GW Hz)	GW slope (dB/Octave)	GW width Q-factor
D02	4	14.1	4.37	0.46	813	18.57	13.29
	8	18.6	2.31	1.02	1 431	10.49	6.44
	12	17.4	3.42	3.30	2 215	12.82	2.04
D05	4	19.3	0.84	6.05	855	3.84	0.99
	8	20.8	1.17	4.92	1 387	5.25	1.30
	12	17.5	2.44	1.79	3 975	11.79	3.89
D08	4	15.4	1.67	3.08	881	7.20	2.00
	8	16.7	2.10	2.42	1 763	9.66	2.76
	12	11.7	2.42	1.57	3 174	11.57	4.39
D19	4	23.7	1.02	5.22	1 033	4.62	1.18
	8	17.8	1.63	1.49	1 737	7.29	4.46
	12	20.9	1.12	3.61	3 413	5.00	1.90
D26	4	28.5	1.67	3.60	944	7.18	1.73
	8	16.4	1.44	3.20	2 183	6.72	2.10
	12	16.2	1.70	2.43	3 476	8.14	2.85
Group averages by electrode region:							
Apical	Ave	20.2	1.91	3.68	905	8.28	3.84
	s.d.	6.0	1.43	2.16	86	5.95	5.30
Middle	Ave	18.1	1.73	2.61	1 700	7.88	3.41
	s.d.	1.8	0.47	1.54	320	2.16	2.05
Basal	Ave	16.7	2.22	2.54	3 251	9.86	3.02
	s.d.	3.3	0.87	0.90	648	3.24	1.11

TABLE V. Spatial tuning curve parameters in Nucleus N22 implant users.

Subj ID	rEL	Ave Lp (%DRuA)	STC slope (dB/mm)	STC width (mm at Q1dB)	Cf (GW Hz)	GW slope (dB/Octave)	GW width Q-factor
N13	7	14.7	2.97	1.19	1 369	15.84	5.51
	11	19.3	2.79	0.78	2 007	13.03	8.63
	16	17.5	2.59	1.62	2 134	12.14	4.18
N14	6	18.9	3.89	1.60	880	17.02	3.88
	12	14.1	2.78	2.57	1 917	12.92	2.60
	16	16.9	3.99	2.76	3 028	19.10	2.48
N28	5	19.5	2.65	2.68	1 045	11.26	2.36
	12	22.9	2.03	4.19	2 695	9.96	1.62
	20	13.8	2.79	0.88	5 111	13.32	7.95
N32	5	16.9	5.16	0.73	1 207	19.41	8.86
	12	16.8	5.20	3.30	3 755	27.16	2.09
	19	11.6	5.08	1.25	5 037	24.76	5.62
N34	5	12.3	5.28	0.43	1 163	23.50	14.86
	10	16.5	4.76	1.66	1 856	22.17	4.03
	17	9.3	2.12	2.95	3 874	10.93	2.34
Group Averages by Electrode Region:							
Apical	Ave	16.5	3.99	1.32	1 133	17.40	7.09
	s.d.	3.0	1.21	0.88	183	4.51	4.97
Middle	Ave	17.9	3.51	2.50	2 446	17.05	3.79
	s.d.	3.3	1.38	1.34	806	7.28	2.85
Basal	Ave	13.8	3.31	1.89	3 837	16.05	4.51
	s.d.	3.5	1.20	0.92	1 286	5.79	2.34

[1]The denominator in the ratio was either the value for the middle probe level or the highest probe level when only two probe levels were tested. In this way, the relative change in slope or bandwidth could be evaluated as opposed to the absolute change in slope or bandwidth.

Bierer, J. A. (**2007**). "Threshold and channel interaction in cochlear implant users: evaluation of the tripolar electrode configureation," J. Accoust. Soc. Am. **121**, 1642–1653.

Bierer, J. A., and Faulkner, K. F. (**2010**). "Identifying cochlear implant channels with poor electrode-neuron interface: Partial tripolar, single-channel thresholds, and psychophysical tuning curves," Ear Hear. **31**, 247–258.

Black, R. C. Clark, G. M. Tong, Y. C., and Patrick, J. F. (**1983**). "Current distribution in cochlear stimulation," Ann. N.Y. Acad. Sci. **405**, 137–145.

Boex, C. Kos, M.-I., and Pelizzone, M. (**2003**). "Forward masking in different cochlear implant systems," J. Acoust. Soc. Am. **114**, 2058–2065.

Bonham, B. H., and Litvak, L. M. (**2008**). "Current focusing and steering: Modeling, physiology, and psychophysics," Hear. Res. **242**, 141–153.

Boothroyd, A. (**1967**). "Discrimination by partially hearing children of frequency distorted speech," Int. J. Audiol. **6**, 136–145.

Cohen, L. T., Richardson, L. M., Saunders, E., and Cowan, R. (**2003**). "Spatial spread of neural excitation in cochlear implant recipients: Comparison of improved ECAP method and psychophysical forward masking," Hear. Res. **179**, 72–87.

Dallos, P., and Harris, D. (**1978**). "Properties of auditory nerve responses in the absence of outer hair cells," J. Neurophysiol. **41**, 365–383.

Donaldson, G. S., Dawson, P. K., and Borden, L. Z. (**2011**). "Within-subjects comparison of the HiRes and Fidelity120 speech processing strategies: Speech perception and its relation to place-pitch sensitivity," Ear Hear. **32**, 238–250.

Donaldson, G. S., and Nelson, D. A. (**2000**). "Place-pitch sensitivity and its relation to consonant recognition by cochlear implant listeners using the MPEAK and SPEAK speech processing strategies," J. Acoust. Soc. Am. **107**, 1645–1658.

Finley, C., Wilson, B., and White, M. (**1990**). "Models of neural responsiveness to electrical stimulation," in *Cochlear Implants. Models of the Electrically Stimulated Ear*, edited by J. M. Miller and F. A. Spelman (Springer-Verlag, New York), pp. 55–96.

French, N. R., and Steinberg, J. C. (**1947**). "Factors governing the intelligibility of speech sounds," J. Acoust. Soc. Am. **19**, 90–119.

Frijns, J. H., Briaire, J. J., de Laat, J. A., and Grote, J. J. (**2002**). "Initial evaluation of the Clarion CII cochlear implant: speech perception and neural response imaging.," Ear Hear. **23**, 184–197.

Glasberg, B. R., and Moore, B. C. J. (**1990**). "Derivation of auditory filter shapes from notched-noise data," Hear. Res. **47**, 103–138.

Greenwood, D. D. (**1990**). "A cochlear frequency-position function for several species - 29 years later," J. Acoust. Soc. Am. **87**, 2592–2605.

Hillenbrand, J., Getty, L. A., Clark, M. J., and Wheeler, K. (**1995**). "Acoustic characteristics of American English Vowels," J. Acoust. Soc. Am. **97**, 3099–3111.

Houtgast, T. (**1973**). "Psychophysical experiments on 'tuning curves' and 'two-tone inhibition'," Acustica **29**, 168–179.

Hughes, M. L., and Stille, L. J. (**2009**). "Psychophysical and physiological measures of electrical-field interaction in cochlear implants," J. Accoust. Soc. Am. **125**, 247–260.

IEEE (**1969**). "IEEE recommended practice for speech quality measurements," Trans. Audio Electroacoust. **17**, 225–246.

Kessler, D. K. (**1999**). "The CLARION Multi-strategy cochlear implant," Ann. Otol. Rhinol. Laryngol. Suppl. **177**, 8–16.

Ketten, D. R., Skinner, M. W., Wang, G., Vannier, M. W., Gates, G. A., and Neely, J. G. (**1998**). "In vivo measures of cochlear length and insertion depth of nucleus cochlear implant electrode arrays," Ann. Otol. Rhinol. Laryngol. **107**, 1–16.

Kluk, K., and Moore, B. C. J. (**2006**). "Detecting dead regions using psychophysical tuning curves: A comparison of simultaneous and forward masking," Int. J. Aud. **45**, 463–476.

Kral, A., Hartmann, R., Mortazavi, D., and Klinke, R. (**1998**). "Spatial resolution of cochlear implants: The electrical field and excitation of auditory afferents," Hear. Res. **121**, 11–28.

Kwon, B.J. and van den Honert, C. (**2006**). "Effect of electrode configuration on psychophysical forward masking in cochlear implant listeners," J. Acoust. Soc. Am. **119**, 2994–3002.

Landsberger, D. M., and Sirinivasan, A. G. (**2009**). "Virtual channel discrimination is improved by current focusing in cochlear implant recipients," Hear. Res. **254**, 34–41.

Levitt, H. (**1971**). "Transformed up-down methods in psychoacoustics," J. Acoust. Soc. Am. **49**, 467–477.

Liang, D. H., Lusted, H. S., and White, R. L. (**1999**). "The nerve-electrode interface of the cochlear implant: Current spread," IEEE Trans. Biomed. Eng. **46**, 35–43.

Liberman, M. C., and Dodds, L. W. (**1984**). "Single-neuron labeling and chronic cochlear pathology. III. Stereocilia damage and alterations of the threshold tuning curves," Hear. Res. **16**, 55–74.

Marsh, M. A., Xu, J., Blamey, P. J., Whitford, L. A., Xu, S. A., Silverman, J. M., and Clark, G. M. (**1993**). "Radiological evaluation of multiple-channel intracochlear implant insertion depth," Am. J. Otol. **14**, 386–391.
Miller, G. A., and Nicely, P. E. (**1955**). "An analysis of perceptual confusions among some English consonants," J. Acoust. Soc. Am. **27**, 338–352.
Moore, B. C. J. (**1978**). "Psychophysical tuning curves measured in simultaneous and forward masking," J. Acoust. Soc. Am. **63**, 524–532.
Moore, B. C. J., and Alcantara, J. I. (**2001**). "The use of psychophysical tuning curves to explore dead regions in the cochlea," Ear Hear. **22**, 268–278.
Nelson, D. A. (**1991**). "High-level psychophysical tuning curves: Forward masking in normal-hearing and hearing-impaired listeners," J. Speech Hear. Res. **34**, 1233–1249.
Nelson, D. A., and Donaldson, G. S. (**2002**). "Forward-masked spatial tuning curves in cochlear implant subjects.," Abstracts of the 25th ARO Midwinter Mtg., 466.
Nelson, D. A., Donaldson, G. S., and Kreft, H. A. (**2008**). "Forward-masked spatial tuning curves in cochlear implant users," J. Acoust. Soc. Am. **123**, 1522–1543.
Nelson, D. A., and Schroder, A. C. (**1997**). "Linearized response growth inferred from growth-of-masking slopes in ears with cochlear hearing loss," J. Acoust. Soc. Am. **101**, 2186–2201.
Nelson, D. A., and Schroder, A. C. (**1999**). "Forward masking recovery and peripheral compression in normal- hearing and cochlear-impaired ears," J. Acoust. Soc. Am. **106**, 2176(A).
Nelson, D.A., and Schroder, A. C. (**2004**). "Peripheral compression as a function of stimulus level and frequency region in normal-hearing listeners," J. Acoust. Soc. Am. **115**, 2221–2233.
Nelson, D. A., Schroder, A. C., and Wojtczak, M. (**2001**). "A new procedure for measuring peripheral compression in normal-hearing and hearing-impaired listeners," J. Acoust. Soc. Am. **110**, 2045–2064.
O'Loughlin, B. J., and Moore, B. C. J. (**1981**). "Off-frequency listening: Effects on psychoacoustical tuning curves obtained in simultaneous and forward masking," J. Acoust. Soc. Am. **69**, 1119–1125.
Oxenham, A. J., and Shera, C. A. (**2003**). "Estimates of human cochlear tuning at low levels using forward and simultaneous masking," J. Assoc. Res. Otolaryngol. **4**, 541–554.
Patrick, J. F., and Clark, G. M. (**1991**). "The Nucleus 22-channel cochlear implant system," Ear Hear. **12**, Suppl., 3S–9S.
Ruggero, M. A. (**1992**). "Responses to sound of the basilar membrane of the mammalian cochlea," Curr. Opin. Neurobiol. **2**, 449–456.
Schindler, R. A., and Kessler, D. K. (**1993**). "Clarion cochlear implant: phase I investigation results," Am. J. Otol. **14**, 263–272.
Seldon, H. L. (**1991**). "Three-dimensional reconstruction of temporal bone from CT scans on a personal computer," Arch. Otolaryngol. Head Neck Surg. **117**, 1158–1161.
Shannon, R. V., Jensvold, A., Padilla, M., Robert, M. E., and Wang, X. (**1999**). "Consonant recordings for speech testing," J. Acoust. Soc. Am. **106**, L71–L74.
Shera, C. A., Guinan, J. J., Jr., and Oxenham, A. J. (**2002**). "Revised estimates of human cochlear tuning from otoacoustic and behavioral measurements," Proc. Natl. Acad. Sci. U. S. A. **99**, 3318–3323.
Skinner, M. W., Ketten, D. R., Holden, L. K., Harding, G. W., Smith, P. G., Gates, G. A., Neely, J. G., Kletzker, G. R., Brunsden, B., and Blocker, B. (**2002**). "CT-Derived estimation of cochlear morphology and electrode array position in relation to word recognition in Nucleus-22 recipients," JARO Online **27**.
Snyder, R., Middlebrooks, J., and Bonham, B. (**2008**). "Cochlear implant electrode configuration effects on activation threshold and tonotopic selectivity," Hear. Res. **235**, 23–38.
Turner, C. W., Burns, E. M., and Nelson, D. A. (**1983**). "Pure tone pitch perception and low-frequency hearing loss," J. Acoust. Soc. Am. **73**, 966–975.
Vogten, L. L. M. (**1978**). "Low-level pure-tone masking: A comparison of 'tuning curves' obtained with simultaneous and forward masking," J. Acoust. Soc. Am. **63**, 1520–1527.
Wang, G., Vannier, M. W., Skinner, M. W., Kalender, W. A., Polacin, A., and Ketten, D. R. (**1996**). "Unwrapping cochlear implants by spiral CT," IEEE Trans. Biomed. Eng. **43**, 891–900.
Zeng, F. G., and Shannon, R. V. (**1992**). "Loudness balance between electric and acoustic stimulation," Hear. Res. **60**, 231–235.
Zwolan, T. A., Collins, L. M., and Wakefield, G. H. (**1997**). "Electrode discrimination and speech recognition in postlingually deafened adult cochlear implant subjects," J. Acoust. Soc. Am. **102**, 3673–3685.